NIH Public Access
Author Manuscript
Inorg Chem. Author manuscript; available in PMC 2006 July 13.

Published in final edited form as:
Inorg Chem. 2006 July 10; 45(14): 5284–5290.

Electronic, Magnetic, and Structural Characterization of the Five-Coordinate, High-Spin Iron(II) Nitrato Complex [Fe(TpivPP)(NO_3)]$^-$

Habib Nasri[†], **Mary K. Ellison**[‡], **Ben Shaevitz**[§], **Govind P. Gupta**[§], and **W. Robert Scheidt**[*,‡]

Abstract

The preparation and characterization of the five-coordinate iron(II) porphyrinate derivative [Fe(TpivPP)(NO_3)]$^-$ (TpivPP = picket fence porphyrin) is described. Structural and magnetic susceptibility data support a high-spin state (S = 2) assignment for this species. The anionic axial nitrate ligand is oxygen-bound, through a single oxygen atom, with an Fe-O bond length of 2.069(4) Å. The planar nitrate ligand bisects an N_p-Fe-N_p angle. The average iron-nitrogen bond length is 2.070(16) Å. The iron atom is located 0.49 Å out of the 24-atom mean porphyrin plane toward the nitrate ligand. From solid-state Mössbauer data, the isomer shift of 0.98 mm/s at 77 K is entirely consistent with high-spin iron(II). However the quadrupole splitting of 3.59 mm/s at 77 K is unusually high for iron(II), S = 2 systems, but within the range of other five-coordinate high-spin ferrous complexes with a single anionic axial ligand. Crystal data for [K(222)][Fe(TpivPP)(NO_3)].C_6H_5Cl: a = 17.888 (5) Å, b = 21.500 (10) Å, c = 22.514 (11) Å, and β = 100.32 (3)° , monoclinic, space group $P2_1/n$, V = 8519 Å ^{3}, Z = 4.

Introduction

The interaction of the nitrogen oxide ligands nitrosyl, nitrite, and nitrate with heme proteins is of great biological importance. Of key interest is the interconversion between these three species in both the nitrogen cycle and mammalian physiology. Despite the progress in the understanding of these important biological functions, many of the intermediates and pathways involving nitrogen oxide ligands are not known. Certainly all of the mechanistic details of the oxidation and reduction process involving these NO_x species are not completely understood. For example, NO is an essential signaling molecule for a variety of physiological functions which include neurotransmission, platelet aggregation, and vasodilation. The production of NO by nitric oxide synthase, leads to activation of guanylyl cyclase which eventually leads to smooth muscle relaxation. The method of NO *depletion* in blood either involves NO binding to the iron proteins, hemoglobin and myoglobin to give HbNO [1-3] and MbNO which can get oxidized by molecular oxygen to give nitrate *or* NO can interact with ferrous MbO_2 and HbO_2 to give nitrate and iron(III) species.[4,5] In fact, the levels of nitrate found in urine can be used as an indication of NO production.[6] Although the binding of NO to oxymyoglobin or oxyhemoglobin can also yield nitrate-coordinated heme derivatives, no structural information on a protein containing a coordinated nitrate ligand has been reported.

For three decades we have been studying the interesting and quite variable bonding capabilities of a number of nitrogen oxide ligands to both iron(II) and iron(III) porphyrin complexes because of their relevance to the structure and function of hemoproteins. The use of X-ray

[†]Faculté des Sciences de Monastir
[‡]University of Notre Dame
[§]The Pennsylvania State University
[*]To whom correspondence should be addressed, e-mail: scheidt.1@nd.edu

Supporting Information Available: Tables S1-S6 giving complete crystallographic information. This material is available free of charge via the Internet at http://pubs.acs.org.

NIH-PA Author Manuscript
NIH-PA Author Manuscript
NIH-PA Author Manuscript

NIH-PA Author Manuscript

NIH-PA Author Manuscript

NIH-PA Author Manuscript

crystallography and EPR and Mössbauer spectroscopies to study these species have been instrumental in defining both the bonding and electronic structure at iron. We have successfully characterized both five- and six-coordinate formally ferric and ferrous porphyrinato nitrosyl complexes of the general formulas $[Fe(Porph)(NO)]^{+}$,[7,8] $[Fe(Porph)(NO)(L)]^{+}$,[9] [Fe(Porph)-(NO)],[10,11] and [Fe(Porph)(NO)(L)] [12-14] which were all found to be low-spin species. Also characterized are iron(II) nitrite species of the general formulas, $[Fe(TpivPP)(NO_2)]^{-}$ [15] and $[Fe(TpivPP)(NO_2)(L)]^{-}$ [16] which are also low spin although the π-bonding ability of nitrite appears to be quite variable. The six-coordinate iron(III) nitrite species $[Fe(TpivPP)(NO_2)(L)]$, [17] and $[Fe(TpivPP)(NO_2)_2]^{-}$ [18] are low spin and the five-coordinate iron(III) nitrite species $[Fe(TpivPP)(NO_2)]$,[19] detected in solution with EPR, was found to be low spin as well. However, the iron(III) nitrate derivatives, $[Fe(Porph)(NO_3)]$,[19-22] are all high spin despite the various modes of binding of the nitrate ligand.

The resulting structural and electronic information from the body of work on these nitrosyl, nitrite and nitrate iron porphyrin complexes have provided great insight into the many biologically relevant processes which involve nitrogen oxide ligands. In further exploration of the issues involved in bonding and geometric and electronic structure we report the synthesis and characterization of a new iron(II) nitrate porphyrin species, $[Fe(TpivPP)(NO_3)]^{-}$.

Experimental Section

General Information. UV-vis spectra were recorded on a Perkin-Elmerg Lambda 4C spectrometer. Magnetic susceptibility measurements were made on a model 905 SHE Corp. SQUID susceptometer at 2 and 10 kG. Field calibration was checked at 0.1 and 1.0 T with a chemical standard of known Curie law behavior.[23] The $[K(222)][Fe(TpivPP)(NO_3)]\cdot C_6H_5Cl$ sample for susceptibility measurements was packed tightly into a preweighed and precalibrated aluminum bucket. A typical sample size was 35 mg. The diamagnetic correction for the picket fence porphyrin was calculated two ways: i) to the observed diamagnetic correction value of H_2TPP[24] (-700×10^{-6} cgsμ) was added the diamagnetic correction of the remaining four pivaloyl groups using Pascal's constants, or ii) the diamagnetic correction was calculated by individually adding the diamagnetic contribution of each atom using Pascal's constants. The diamagnetic correction for $[K(222)][Fe(TpivPP)(NO_3)]\cdot C_6H_5Cl$ (adding Pascal's constants for the remaining atoms) by the first method is -1304.15×10^{-6} cgsμ and -967.47×10^{-6} cgsμ using the second method (second method values used). Mössbauer spectra were recorded in horizontal transmission geometry by using a constant-acceleration spectrometer operated in connection with a 256-channel analyzer in the time scale mode as described previously.[25] Mössbauer samples (~75 mg) of $[K(222)][Fe(TpivPP)(NO_3)]\cdot C_6H_5Cl$ were prepared by immobilization of the crystalline material into melted paraffin wax (mp ~78 °C) within a 1 cm diameter Plexiglas dish.

Preparation of $[K(222)][Fe(TpivPP)(NO_3)]\cdot C_6H_5Cl$. All manipulations were carried out under argon using a double manifold vacuum line, Schlenkware, and cannula techniques. Chlorobenzene and benzene were purified by washing with sulfuric acid and then distilled over P_2O_5 or sodium/benzophenone, respectively. These solvents were stored under argon and kept away from light. Pentane was distilled over CaH_2 and used immediately. All solvents were degassed by the freeze-pump-thaw method several times before use. The potassium nitrate was recrystallized twice from distilled water, dried overnight under vacuum, and stored under argon. Kryptofix-222 (Aldrich) was recrystallized from benzene and stored under argon in the dark. The Kryptofix-222 was recrystallized to remove water and especially to remove the halide impurities which are known to readily coordinate to the Fe(II) porphyrin species.[26,27] $[Fe(TpivPP)(SO_3CF_3)(H_2O)]\cdot C_6H_5Cl$ [29] (100 mg, 0.08 mmol) and 1 mL of zinc amalgam were stirred for 1 hour under argon in C_6H_5Cl (10 mL). This deep red solution ([Fe(II)TpivPP]) was then filtered under argon into a second solution that was made by stirring 305 mg of

NIH-PA Author Manuscript

NIH-PA Author Manuscript

NIH-PA Author Manuscript

Kryptofix-222 and 164 mg of KNO_3 (1.6 mmol) in C_6H_5Cl (10 mL) for 12 hours. The bright red-green solution was filtered and crystals prepared by slow diffusion of pentane into the C_6H_5Cl solution. The resulting crystalline material was washed (under argon) with portions of thoroughly degassed water to remove excess KNO_3 and Kryptofix-222 and then washed with several portions of pentane. UV-vis (C_6H_5Cl): λ_{max}, nm (log*[epsilon1]*); 417 (4.70)(sh); 438 (4.93); 534 (3.83)(sh); 564 (4.08); 604 (3.64). IR(KBr): *v* (NO^-_3): 1354 cm^{-1}.

X-ray Diffraction Studies. A single crystal of [K(222)][Fe(TpivPP)(NO_3)]·C_6H_5Cl (0.81 × 0.53 × 0.21 mm^3) was subjected to examination on an Enraf-Nonius CAD4 diffractometer equipped with a locally modified Syntex LT-1 low-temperature attachment to provide a 118 ± 5 K cold stream. All measurements were performed with graphite-monochromated Mo Kα radiation. The crystal was glued to the end of a glass fiber with cyanoacrylate and quickly transferred to the cold stream. Intensity data were measured at low temperature by the θ - 2θ scan method with a constant scan rate of 3° (in θ). The intensity data were reduced with the Blessing program suite[30] with standard Lorentz and polarization corrections but were not corrected for absorption. A total of 10231 reflections having sin θ/λ < 0.576 and $F_o \geq 3.0\sigma(F_o)$ were taken as observed. The structure of [K(222)][Fe(TpivPP)(NO_3)]·C_6H_5Cl was solved in the monoclinic space group, $P\,2_1/n$, using coordinates for the iron, porphyrin and Kryptofix-222 cation from the structure of [Na(222)][Fe(TpivPP)(O_2CCH_3)]·C_6H_5Cl. [31] The remaining axial ligand and solvent atoms were found from a difference Fourier calculation.[32]

After isotropic least-squares refinement had been carried to convergence, difference Fourier syntheses suggested possible locations for all hydrogen atoms. All hydrogen atoms were included in subsequent cycles of least-squares refinement as fixed idealized contributors (C-H = 0.95 Å, N-H = 0.90 Å and B(H) = B(C,N) × 1.3). Final cycles of full-matrix least-squares used anisotropic temperature factors for all heavy atoms. At convergence, $R_1 = 0.074$ and $R_2 = 0.093$, the error of fit was 1.88 and the final data/variable ratio was 20.1. Final difference Fourier maps were judged to be significantly free of features. Complete crystallographic details, atomic coordinates, anisotropic thermal parameters, and fixed hydrogen atom coordinates are included in the Supporting Information.

Results

The synthesis of the iron(II) species, [K(222)][Fe(TpivPP)(NO_3)], involves the addition of [Fe^{II}TpivPP] (made by reduction of the triflate complex, [Fe(TpivPP)(SO_3CF_3)(H_2O)] with zinc amalgam) to excess potassium nitrate solubilized by the cryptand, Kryptofix-222 under strict anaerobic conditions. Both the cryptand and the KNO_3 must be carefully recrystallized to remove halide impurities which bind strongly to iron(II) species. Crystalline [K(222)][Fe(TpivPP)(NO_3)] was then obtained by slow diffusion of pentane into the chlorobenzene solution. This new compound has been characterized by UV-vis and Mössbauer spectroscopies, magnetic susceptibility, and a single-crystal X-ray structure determination.

The molecular structure of [Fe(TpivPP)(NO_3)]$^-$ is illustrated in Figure 1. The iron atom is five coordinate, bound to the four porphyrin nitrogen atoms and to a single oxygen atom of the nitrate ligand. The nitrate ligand is bound inside the pocket formed by the pivalamide groups of the picket fence porphyrin. The monodentate iron-oxygen bond length is 2.069(4) Å and the average equatorial Fe-N_p bond length is 2.070(16) Å. These values and other selected bond lengths are given in Table 1. The individual N-O bond lengths for the nitrate ligand are given in Table 2. The nitrate ligand plane nearly bisects an N_p-Fe-N_p angle as can be seen in Figure 2. Also shown in this figure are the individual iron-porphyrin nitrogen bond lengths and the closest interaction between a pivolyl group of the picket fence porphyrin and the nitrate ligand. There is a hydrogen bond between a nitrate anion oxygen atom and one of the picket amido groups. The N(8)-H(N8)…O(12) hydrogen bond distance is 2.33 Å.

NIH-PA Author Manuscript

NIH-PA Author Manuscript

NIH-PA Author Manuscript

The iron is significantly displaced out of the 24-atom porphyrin plane toward the nitrate ligand by 0.49 Å and by 0.42 Å from the four nitrogen atom plane. The porphyrin core is modestly ruffled and there is a small (0.07 Å) doming toward the nitrate ligand. This information is given in Figure 3. This figure shows the core atom displacements (in units of 0.01 Å) from the 24-atom mean porphyrin plane. Also included in the diagram are the averaged values of the unique bond lengths (Å) and angles (degrees) in the porphyrin core. Individual bond lengths and angles are given in the Supporting Information.

The negative charge of the $[Fe(TpivPP)(NO_3)]^-$ anion is balanced by a potassium-222 counterion. An ORTEP drawing of this counterion is given in Figure 4. The eight-coordinate potassium ion is bonded to six oxygen atoms and two nitrogen atoms. The average K-O(222) distance is 2.82(2) Å and the average K-N(222) bond length is 3.05(2) Å.

Crystalline $[K(222)][Fe(TpivPP)(NO_3)]$ was also studied by solid-state Mössbauer measurements. The quadrupole splitting and isomer shift were found to be 3.59 mm/s and 0.98 mm/s respectively, at 77 K and 3.56 and 0.98 mm/s at 4.2 K. These values of ΔE_Q and δ_{Fe} are given in Table 3 along with Mössbauer data for related iron(II) and iron(III) porphyrin species. The magnetic susceptibility for $[K(222)][Fe(TpivPP)(NO_3)]$ was measured between 1.91 and 302 K. A plot of the magnetic data is shown in Figure 5.

Discussion

Although there are several iron(III) porphyrin nitrate species of the general formula $[Fe(Porph)(NO_3)]$ structurally characterized,[19-22] $[Fe(TpivPP)(NO_3)]^-$ is the first such iron(II) species characterized. The synthesis of $[Fe(TpivPP)(NO_3)]^-$ involves addition of excess KNO_3 solubilized with a cryptand to the four coordinate iron(II) species, [Fe(TpivPP)], under anaerobic conditions. Picket fence porphyrin was used to provide a protective binding pocket thought to reduce the risk of O-atom transfer chemistry known to occur in iron(III) nitrite species.[52] A solution electronic spectrum confirmed the synthesis, and persistence in solution, of a new species with a Soret band at 438 nm in chlorobenzene. The position of the Soret band is red-shifted compared to the iron(III) nitrate species, $[Fe(TPP)(NO_3)]$, which appears at 412 nm in methylene chloride.[20] Similar red shifts are seen when comparing iron(III) vs iron(II) chloride and also acetate species. For instance, the Soret for [Fe(TPP)Cl] is at 417 nm with that for $[Fe(TpivPP)Cl]^-$ at 446 nm[28] and the Soret of $[Fe(TpivPP)(O_2CCH_3)]$ at 414 nm shifts to 448 nm for $[Fe(TpivPP)(O_2CCH_3)]^-$ in chlorobenzene.[31] So, the solution electronic spectrum for $[Fe(TpivPP)(NO_3)]^-$ alone suggests the formation of a new iron(II) porphyrin species. The question of spin state however remains. The five-coordinate, high-spin, neutral species, [Fe(TpivPP)(2-MeHIm)], has a Soret band at 436 nm.[36] As stated above, the high-spin iron(II) halide and oxyanionic (RO^-) species have Soret maxima around 440 nm. Interestingly however, the Soret maximum for the *low-spin* iron(II) anionic species, $[Fe(TpivPP)(NO_2)]^-$, is also in this area at 444 nm.[15,16]

In five-coordinate iron(II) porphyrinates, the nature of the axial ligand determines the spin state. Strong axial ligands such as NO and CS result in low-spin complexes. Weak field ligands such as the halides and imidazoles yield high-spin species. Iron(II) porphyrinates with oxyanionic ligands are either high- or low-spin. For example, nitrite yields an N-bound low-spin species[16] and methoxide,[31] acetate,[42] and phenolate[23] yield high-spin species. So the question remains, will nitrate result in a low-spin or high-spin species?

The molecular structure, specifically the geometry at iron, can be a strong indicator of spin state. For instance, high-spin iron(II) five-coordinate complexes have typical Fe out-of-plane displacements of ≥ 0.5 Å and high-spin six-coordinate species have expanded porphyrin cores. Consequently, the average Fe-N_p bond lengths for high-spin iron(II) complexes are elongated compared to low-spin complexes. The iron atom displacement for $[Fe(TpivPP)(NO_3)]^-$ is 0.49

NIH-PA Author Manuscript

NIH-PA Author Manuscript

NIH-PA Author Manuscript

Å and Fe-N_p is 2.070(16) Å, which is at the low end of the range of Fe-N_p bond lengths for high-spin iron(II) porphyrin complexes (2.07 Å-2.11 Å).[53]

Iron-axial ligand bond lengths are also indicative of spin state. Long Fe-L bond lengths characterize high-spin complexes. In iron(III) porphyrin nitrate complexes, bonding of the axial nitrate ligand is exclusively through oxygen, although the denticity varies greatly. For example, in the two crystalline forms of [Fe(OEP)(NO_3)], the nitrate is bound in a monodentate fashion.[21,22] However, in the triclinic form the Fe-O bond length is significantly longer than in the monoclinic form (confer Table 2). The nitrate ligand in [Fe(TPP)(O_2NO)] is bound in a near symmetrical bidentate fashion.[22] In [Fe(TpivPP)(O_2NO)] the nitrate ligand is bound in a more symmetrical bidentate fashion; that is the two Fe-O bond lengths are nearly equivalent.[19] The large denticity range from monodentate to a nearly symmetrical bidentate fashion in these iron (III) nitrate species results in a large range of Fe-O bond lengths (1.966-2.323 Å). Concurrently, the orientation of the nitrate ligand plane with respect to porphyrin plane also varies greatly. The dihedral angle between the nitrate plane and the closest N_p-Fe-O angle ranges from 10° to 45° (Table 2).

In the iron(II) species, [Fe(TpivPP)(NO_3)]$^-$, the nitrate anion is in the pocket of the picket fence porphyrin as is almost always the case for complexes of the general formula [Fe(TpivPP)(X)]$^{0/-}$, where X is an anionic ligand. The nitrate is bound in a monodentate fashion with the Fe-O(NO_3) vector close to normal to the porphyrin plane and an Fe-O(NO_3) bond length of 2.069(4) Å. This bond length is longer in [Fe(TpivPP)(NO_3)]$^-$ than in the two iron(III) species with monodentate binding of nitrate due to the added electron. As can be seen from Figure 2, the oxygen atom is directly over the iron atom which corresponds to a long Fe‖O(NO_3) distance to the next closest oxygen atom of the nitrate ligand. The ligand plane nearly bisects the two shorter Fe-N_p bonds. In the iron(III) derivative, [Fe(TpivPP)(NO_3)], there are also two long and two short Fe-N_p bonds but the nitrate ligand nearly eclipses the two long bonds which are across from each other.[19] The significance of the varied modes of binding of the nitrate ligand are not clear but likely result in different electronic structures at iron which may in turn affect the reactivity of the different iron species. Although definitive structural data are not available, it appears that some iron(III) porphyrinate species can adopt either monodentate or bidentate nitrate coordination modes. This bidentate nitrate possibility for iron(II) is being explored.

Mössbauer spectroscopy was used to characterize the electronic structure of [Fe(TpivPP)-(NO_3)]$^-$. The typical quadrupole splitting for a six-coordinate low-spin ferrous porphyrin species is ~1 mm/s with decreased values for more π-bonding axial ligands (confer Table 3). These low-spin iron(II) species are also characterized with decreased isomer shifts (δ_{Fe} < 0.5 mm/s). Porphyrin species with isomer shift values of ~0.8-1 mm/s are expected for high-spin iron(II).[54] Indeed, the isomer shift for [Fe(TpivPP)(NO_3)]$^-$ of 0.98 mm/s at 77 K strongly supports a high-spin state assignment for this species. The quadrupole splitting for high-spin iron(II) complexes however, varies greatly. The neutral five-coordinate imidazole species, [Fe(Porph)(RIm)], as well as deoxyhemoglobin and -myoglobin have values for the quadrupole splitting of ~2 mm/s and are negative in sign. The species [Fe(TpivPP)(SC_6HF_4)]$^-$ and [Fe(TpivPP)($THF)_2$] also have the usual, smaller quadrupole splittings of ~2 mm/s. Previous studies[28,31,55,56] suggest that species of the general formula [Fe(Porph)(X)]$^-$ where X is a halide ion, or an anionic oxygen-donor ligand have distinctively large quadrupole splittings (ΔE_Q ~3.5-4 mm/s). Indeed the quadrupole splitting for [Fe(TpivPP)(NO_3)]$^-$ at 3.59 mm/s is consistent with their findings. These unusually large quadrupole splitting values likely arise from a significant bonding orbital contribution to the EFG from the anionic axial ligand and that d_{xy} becomes the lowest d-orbital in energy and hence doubly occupied. Further exploration of possible classes of high-spin iron(II) porphyrinates is in progress.[57]

NIH-PA Author Manuscript

NIH-PA Author Manuscript

NIH-PA Author Manuscript

The $S = 2$ spin state has also been confirmed from the measurement of the temperature-dependent magnetic susceptibility. The limiting value of μ_{eff} is 5.3 μ_B at 302 K, slightly larger than that expected for the spin-only moment. The temperature dependence, displayed in Figure 5, is consistent with a significant zero field splitting parameter of 10 cm^{-1}.

Summary. A new five-coordinate iron(II) anionic porphyrin species has been synthesized and characterized. From the single-crystal structure determination, the nitrate ligand is found to be bound in a monodentate fashion. The large iron out-of-plane displacement and long Fe-N_p bond lengths shows a high-spin state assignment for this species. The magnetic data confirm this assignment. The unusually large quadrupole splitting value found in the Mössbauer spectrum is similar to those found for other species of the type $[Fe(Porph)(X)]^-$ but distinctly different in magnitude and sign than those found for deoxymyoglobin, deoxyhemoglobin, and their model compounds. Since there is no structural information on iron coordinated to nitrate in a protein, even though there are proposed intermediates of such species, the structural and magnetic information gathered here will be of use for characterization of future biologically significant molecules of this type.

Supplementary Material

Refer to Web version on PubMed Central for supplementary material.

Acknowledgements

Acknowledgments. We thank the National Institutes of Health for support of this research under Grants GM-38401 (WRS), and HL-16860 (GL). We thank Prof. C. A. Reed for assistance in obtaining the magnetic susceptibility data.

References and Notes

(1). Abbreviations used in this paper include Porph, a generalized porphyrin dianion; TpivPP, dianion of (α,α,α,α-tetrakis(*o*-pivalamidophenyl)porphyrin; TPP, dianion of *meso*-tetraphenylporphyrin; Piv_2C_8P, dianion of α,α,5,15-[2,2́-(octanediamido)diphenyl]- α,α,10,20-bis(*o*-pivalamidophenyl) porphyrin; OEP, dianion of octaethylporphyrin; T*p*-OCH_3PP, di-anion of *meso*-tetra-*p*-methoxyphenylporphyrin; TMP, dianion of *meso*-tetramesityl porphyrin; TTP, dianion of *meso*-tetratolyl porphyrin; Kryptofix-222 or 222, 4,7,13,16,21,24-hexaoxo-1,10-diazabicyclo[8.8.8] hexacosane; PMS, pentamethylene sulfide; Py, pyridine; Pip, piperidine; 1-VinIm, 1-vinylimidazole; THF, tetrahydrofuran; 1-MeIm, 1-methylimidazole; 2-MeIm, 2-methylimidazole; 1,2-Me_2Im, 1,2-dimethylimidazole; N_p, porphyrinato nitrogen; Hb, hemoglobin; Mb, myoglobin.

(2). Vandegriff, KD.; Winslow, RM. “Blood Substitutes: Physiological Basis of Efficacy”. Winslow, RM.; Vandegriff, KD.; Intaglietta, M., editors. Birkauser; Boston: 1995. p. 143-154.

(3). Inoue M, Minamiyama Y, Takemura S. Methods Enzymol 1996;269:474. [PubMed: 8791676]

(4). Doyle MP, Hoekstra JW. J. Inorg. Biochem 1981;14:351. [PubMed: 7276933]

(5). Eich RF, Li T, Lemon DD, Doherty DH, Curry SR, Aitken JF, Mathews AJ, Johnson KA, Smith RD, Phillips GN.

(6). Granger DL, Taintor RR, Boockvar KS, Hibbs JB. Methods Enzymol 1996;268:142. [PubMed: 8782580]

(7). Scheidt WR, Lee YJ, Hatano K. J. Am. Chem. Soc 1984;106:3191.

(8). Ellison MK, Schulz CE, Scheidt WR. Inorg. Chem 2000;39:5102. [PubMed: 11233208]

(9). Ellison MK, Scheidt WR. J. Am. Chem. Soc 1999;121:5210.

(10). Scheidt WR, Frisse ME. J. Am. Chem. Soc 1975;97:17. [PubMed: 1133330]

(11). Nasri H, Haller KJ, Wang Y, Huynh BH, Scheidt WR. Inorg. Chem 1992;31:3459.

(12). Piciulo PL, Rupprecht G, Scheidt WR. J. Am. Chem. Soc 1974;96:5293.

(13). Scheidt WR, Brinegar AC, Ferro EB, Kirner JF. J. Am. Chem. Soc 1977;99:7315.

(14). Wyllie GRA, Schulz CE, Scheidt WR. Inorg. Chem 2003;42:5722. [PubMed: 12950223]

(15). Nasri H, Wang Y, Huynh BH, Scheidt WR. J. Am. Chem. Soc 1991;113:717.

NIH-PA Author Manuscript NIH-PA Author Manuscript NIH-PA Author Manuscript

(16). Nasri H, Ellison MK, Krebs C, Huynh BH, Scheidt WR. J. Am. Chem. Soc 2000;122:10795.

(17). Nasri H, Wang Y, Huynh BH, Walker FA, Scheidt WR. Inorg. Chem 1991;30:1483.

(18). Nasri H, Goodwin JA, Scheidt WR. Inorg. Chem 1990;29:185.

(19). Munro OQ, Scheidt WR. Inorg. Chem 1998;37:2308. [PubMed: 11670389]

(20). Phillippi MA, Baenziger N, Goff HM. Inorg. Chem 1981;20:3904.

(21). Ellison MK, Shang M, Kim J, Scheidt WR. Acta Crystallogr., Sect. C 1996;C52:3040. [PubMed: 9015894]

(22). Wyllie GRA, Munro OQ, Schulz CE, Scheidt WR. ms. in preparation.

(23). Shaevitz BA, Lang G, Reed CA. Inorg. Chem 1988;27:4607.

(24). Eaton SS, Eaton GR. Inorg. Chem 1980;19:1095.

(25). Mashiko T, Kastner ME, Spartalian K, Scheidt WR, Reed CA. J. Am. Chem. Soc 1978;100:6354.

(26). Schappacher M, Weiss R, Montiel-Montoya R, Trautwein A, Tabard A. J. Am. Chem. Soc 1985;107:3736.

(27). At the beginning of our investigation, before an adequate recrystallization of the Kryptofix-222 and KNO_3 was performed, an impure Fe(II) porphyrin species was crystallized. X-ray studies at *-150* °C showed that crystals of this species belonged to the triclinic system with *a* = 12.882 (8) Å, *b* = 14.324 (13) Å, *c* = 24.191 (13) Å, α = 81.03 (6)°, β = 80.85 (5)°, γ = 87.17 (6)°, space group *P*, and Z = 2. Preliminary results (R_1 = 12.2%) indicated an iron picket fence porphyrin complex bonded to the oxygen atom of a nitrate ion. However, this ion was present only approximately 75% of the time. This nitrate oxygen atom had an Fe-O distance of 2.13 Å, (using rigid group refinement methods), the remaining 25% of the axial ligand to iron is likely a chloride ion with Fe-Cl = 2.23 Å. This mixture was confirmed by a Mössbauer spectrum, which showed the presence of a second high-spin Fe(II) (impurity) with a quadrupole splitting of 4.29 $mm.s^{-1}$, a value very close to what was found for $[Fe(II)(TpivPP)(Cl)]^-$ (ΔE_Q = 4.36 mm/s at 77K). 28 Interestingly, both of these species, as *pure end members*, crystallize in the monoclinic system, and are effectively isomorphous.

(28). Schappacher M, Ricard L, Weiss R, Montiel-Montoya R, Gonser U, Bill E, Trautwein AX. Inorg. Chim. Acta 1983;78:L9–L12.

(29). Nasri, H. Ph.D Thesis. Univ. Louis Pasteur; Strasbourg, France: 1987.

(30). Blessing RH. Crystallogr. Rev 1987;1:3.

(31). Nasri H, Fischer J, Weiss R, Bill E, Trautwein A. J. Am. Chem. Soc 1987;109:2549.

(32). Cromer DT, Mann JB. Acta Crystallogr., Sect. A 1968;24:321.Cromer DT, Liberman DJ. J. Chem. Phys 1970;53:1891.Stewart RF, Davidson ER, Simpson WT. Ibid 42:3175.

(33). Mandon D, Ott-Woelfel F, Fischer J, Weiss R, Bill E, Trautwein AX. Inorg. Chem 1990;29:2442.

(34). Caron C, Mitschler A, Riviere G, Schappacher M, Weiss RJ. Am. Chem. Soc 1979;101:7401.

(35). Schappacher M, Ricard L, Fischer J, Weiss R, Montiel-Montoya R, Bill E, Trautwein AX. Inorg. Chem 1989;28:4639.

(36). Jameson GB, Molinaro FS, Ibers JA, Collman JP, Brauman JI, Rose E, Suslick KS. J. Am. Chem. Soc 1980;102:3224.

(37). Collman, JP.; Kim, N.; Hoard, JL.; Lang, G.; Radonovich, LJ.; Reed, CA. 167th National Meeting of the American Chemical Society; Los Angeles, CA. April 1974; Washington, D. C.: American Chemical Society; Abstracts of PapersINOR 29

(38). Ellison MK, Schulz CE, Scheidt WR. Inorg. Chem 2002;41:2173. [PubMed: 11952371]

(39). Momenteau M, Scheidt WR, Eigenbrot CW, Reed CA. J. Am. Chem. Soc 1988;110:1207.

(40). Scheidt WR, Geiger DK. Inorg. Chem 1982;21:1208.

(41). Reed CA, Mashiko T, Scheidt WR, Spartalian K, Lang GJ. Am. Chem. Soc 1980;102:2302.

(42). Bominaar EL, Ding X-Q, Gismelseed A, Bill E, Winkler H, Trautwein AX, Nasri H, Fischer J, Weiss R. Inorg. Chem 1992;31:1845.

(43). Boso B, Lang G, Reed CA. J. Chem. Phys 1983;78:2561.

(44). Kent TA, Spartalian K, Lang G, Yonetani T, Reed CA, Collman JP. Biochem. Biophys. Acta 1979;580:245. [PubMed: 518901]

(45). Hu C, Roth A, Ellison MK, An J, Ellis CM, Schulz CE, Scheidt WR. J. Am. Chem. Soc 2005;127:5675. [PubMed: 15826208]

NIH-PA Author Manuscript

NIH-PA Author Manuscript

NIH-PA Author Manuscript

(46). Safo MK, Nesset MJM, Walker FA, Debrunner PG, Scheidt WR. J. Am. Chem. Soc 1997;119:9438.
(47). Kobayashi H, Maeda Y, Yanagawa Y. Bull. Chem. Soc. Jpn 1970;43:2342.
(48). Dolphin D, Sams JR, Tsin TB, Wong KL. J. Am. Chem. Soc 1976;98:6970. [PubMed: 965659]
(49). Safo MK, Scheidt WR, Gupta GP. Inorg. Chem 1990;29:626.
(50). Collman JP, Hoard JL, Kim N, Lang G, Reed CA. J. Am. Chem. Soc 1975;97:2676. [PubMed: 166106]
(51). Polam JR, Wright JL, Christensen KA, Walker FA, Flint H, Winkler H, Grodzicki M, Trautwein AX. J. Am. Chem. Soc 1996;118:5272.
(52). Finnegan MG, Lappin AG, Scheidt WR. Inorg. Chem 1990;29:181.
(53). Scheidt, WR. Systematics of the Stereochemistry of Porphyrins and Metalloporphyrins. In: Kadish, KM.; Smith, K.; Guilard, R., editors. The Porphyrin Handbook. 3. Academic Press; San Diego, CA and Burlington, MA: 2000. Chapter 16
(54). Debrunner, PG. Iron Porphyrins. Lever, ABP.; Gray, HB., editors. VCH Publishers Inc.; New York: 1983. Part 3Chapter 2
(55). Silver J, Lukas B. Inorg. Chim. Acta 1983;80:107.
(56). Silver J, Lukas B, Al-Jaff G. Inorg. Chim. Acta 1984;91:125.
(57). Scheidt WR, Hu C, Schulz CE. work in progress.

NIH-PA Author Manuscript

NIH-PA Author Manuscript

NIH-PA Author Manuscript

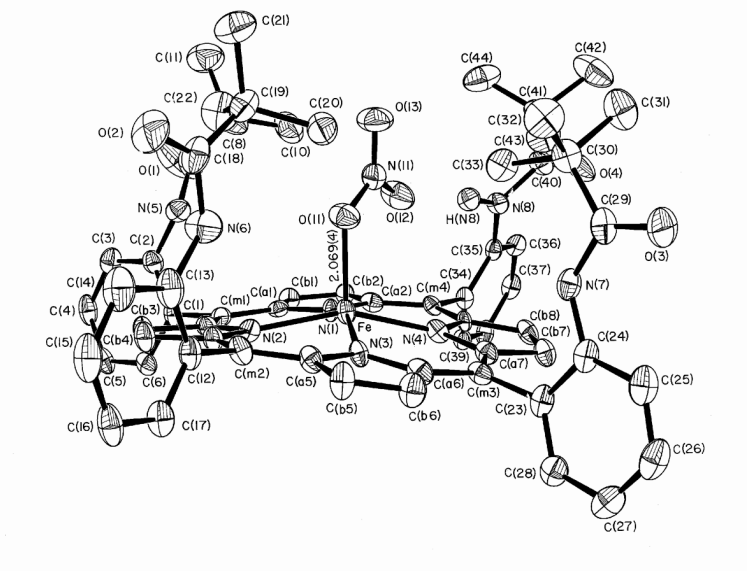

Figure 1.

ORTEP diagram of $[Fe(TpivPP)(NO_3)]^-$ showing the position of the nitrate ligand in the pocket of the picket fence porphyrin. Thermal probability ellipsoids are drawn at the 50% level. Hydrogen atoms have been omitted for clarity except for the amide hydrogen atom nearest the nitrate ligand.

NIH-PA Author Manuscript

NIH-PA Author Manuscript

NIH-PA Author Manuscript

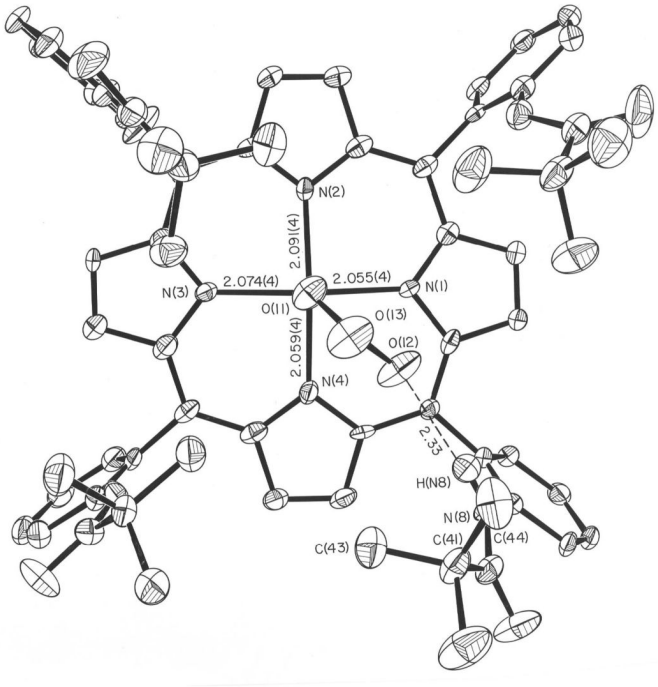

Figure 2.
ORTEP diagram of $[Fe(TpivPP)(NO_3)]^-$ looking onto the porphyrin plane from the pocket side of the picket fence porphyrin. Selected bond lengths are given (in Å).

NIH-PA Author Manuscript

NIH-PA Author Manuscript

NIH-PA Author Manuscript

Figure 3.
Formal diagram of the porphyrinato core of $[Fe(TpivPP)(NO_3)]^-$. Illustrated are the displacements of each atom from the mean plane of the 24-atom core in units of 0.01 Å. Positive values of displacement are toward the nitrate ligand. The diagram also gives the averaged values of each distinct bond distance and angle in the porphyrinato core.

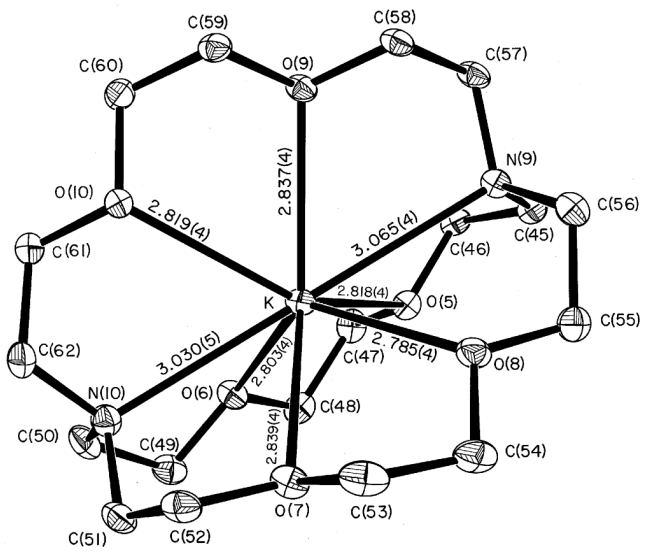

Figure 4.
ORTEP diagram of the K(222) cation. Thermal probability ellipsoids are drawn at the 50% level. Hydrogen atoms have been omitted for clarity.

NIH-PA Author Manuscript NIH-PA Author Manuscript NIH-PA Author Manuscript

NIH-PA Author Manuscript

NIH-PA Author Manuscript

NIH-PA Author Manuscript

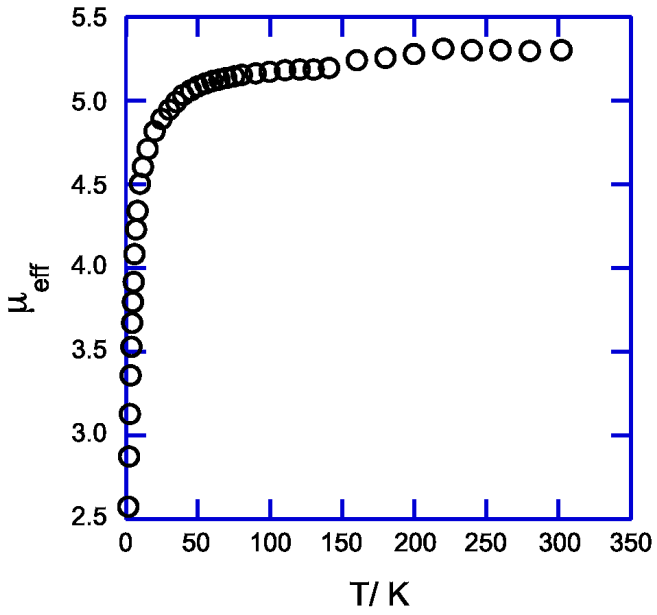

Figure 5.
Magnetic susceptibility of [K(222)][Fe(TpivPP)(NO_3)] over the temperature range of 1.91 to 302 K.

NIH-PA Author Manuscript

NIH-PA Author Manuscript

NIH-PA Author Manuscript

Table 1.

Selected Bond Parameters (Å) for Five-coordinate Iron(II) Porphyrin Derivatives

Iron(II) Complex	Fe-Np	Fe-L	ΔN_4[a]	Δ[b]	Ct…N	S	ref
[Fe(TpivPP)(NO_3)]$^-$	2.070(16)	2.069(4)	0.42	0.49	2.027	2	this work
[Fe(TpivPP)Cl]$^-$	2.108(15	2.301(2)	0.53	0.59	2.040	2	28
[Fe(TpivPP)Br]$^-$	2.094(3)	2.434(2)	0.49	NR	2.036	2	29
[Fe(TpivPP)I]$^-$	2.079(2)	2.712(1)	0.40	NR	2.040	2	29
[Fe(TpivPP)(2-MeIm$^-$)]$^-$	2.11(2)	2.002(15)	0.52	0.65	2.045	2	33
[Fe(TpivPP)(SC_6HF_4)]$^-$	2.076(20)	2.370(3)	0.42	NR	2.033	2	28
[Fe(TPP)(SC_2H_5)]	2.096(4)	2.360(2)	0.52	0.62	2.030	2	34
[Fe(TpivPP)(SC_2H_5)]$^-$	2.074(10)	2.324(2)	0.44	0.52	2.027	2	35
[Fe(TpivPP)(O_2CCH_3)]$^-$	2.107(2)	2.034(3)	0.55	0.64	2.033	2	31
[Fe(TpivPP)(OC_6H_5)]$^-$	2.114(2)	1.937(4)	0.56	0.62	2.037	2	31
[Fe(TpivPP)(NO_2)]$^-$	1.970(4)	1.849(6)	NR	0.18	1.962	0	15,16
[Fe(TpivPP)(2-MeHIm)]	2.072(6)	2.095(6)	0.40	0.43	2.033	2	36
[Fe(TPP)(2-MeHIm)](2-fold)	2.086(8)	2.161(5)	0.42	0.55	2.044	2	37
[Fe(TPP)(2-MeHIm)] ·1.5C_6H_5Cl	2.073(9)	2.127(3)[c]	0.32	0.38	2.049	2	38
[Fe(Piv_2C_8P)(1-MeIm)]	2.075(20)	2.13(2)	0.31	0.34	2.051	2	39
[Fe(OEP)(CS)]	1.982(5)	1.662(3)	0.22	0.23	1.970	0	40
[Fe(TPP)(NO)]	2.001(3)	1.717(7)	0.21	0.21	1.990	0	10
[Fe(TPP)($THF)_2$]	2.057(4)	2.351(3)	0.0[d]	0.0[d]	2.057	2	41

[a] Displacement of iron from the mean plane of the four pyrrole nitrogen atoms.

[b] Displacement of iron from the 24-atom mean plane of the porphyrin core.

[c] Major imidazole orientation.

[d] Six-coordinate; required to be zero by symmetry.

NIH-PA Author Manuscript

NIH-PA Author Manuscript

NIH-PA Author Manuscript

Table 2.

Summary of Bond Parameters for Iron(II) and Iron(III) Nitrate-Coordinated Porphyrin Derivatives

Iron Complex	Fe-Npa	Fe-O(NO3)[a]	N-O[a]	Δ[b]	φ,[cd]	ref
[Fe(TpivPP)(ONO_2)]$^-$	2.070(16)	2.069(4)[e]	1.283(6) 1.230(6)	0.49	45	this work
[Fe(OEP)(ONO_2)][f]	2.056(1)	2.016 2.64	1.232(6) 1.206(5) 1.198(4)	0.50	31	21
[Fe(OEP)(ONO_2)][g]	2.047(6)	1.966(2)[e] 3.042	1.208(6) 1.301(3) 1.212(3)	0.45	41	22
[Fe(TPP)(O_2NO)]	2.085(10)	2.125(3)[h] 2.268(4)	1.199(3) 1.199(4) 1.300(3)	0.62	13	22
[Fe(TpivPP)(O_2NO)]	2.071(14)	2.123(3)[h] 2.226(3)	1.217(3) 1.271(4) 1.252(4) 1.214(3)	0.61	10	19

[a] Value in Å.

[b] Displacement of iron from the 24-atom mean plane of the porphyrin core.

[c] Value in degrees.

[d] Dihedral angle between the nitrate plane and the closest O-Fe-Np plane.

[e] Monodentate.

[f] Triclinic form.

[g] Monoclinic form.

[h] Bidentate.

NIH-PA Author Manuscript

NIH-PA Author Manuscript

NIH-PA Author Manuscript

Table 3.

Solid-State Mössbauer Parameters for[Fe(TpivPP)(NO_3)]$^-$ and Related Derivatives

	ΔEQ,mm/s	δFe, mm/s	T, K	ref
High-Spin Iron(II) Complexes				
[Fe(TpivPP)(NO_3)]$^-$	3.59	0.98	77	tw
[Fe(TpivPP)(OCH_3)]$^-$	3.64	1.00	77	31
[Fe(TpivPP)(OC_6H_5)]$^-$	3.86	1.04	77	31
[Fe(TpivPP)(O_2CCH_3)]$^-$	4.19	1.03	77	31
[Fe(TpivPP)(O_2CCH_3)]$^-$	4.25	1.05	4.2	42
[Fe(TPP)(OC_6H_5)]$^-$	4.01	1.03	4.2	23
[Fe(TpivPP)(Cl)]$^-$	4.36	1.01	77	28
[Fe(TpivPP)(SC_6HF_4)]$^-$	2.37	0.82	85	28
[Fe(TPP)($THF)_2$]	2.75	0.96	77	43
[Fe(TPP)(2-MeHIm)]	2.40	0.92	4.2	38
[Fe(TPP)(2-MeHIm)](2-fold)	2.28	0.93	4.2	44
[Fe(TPP)(1,2-Me_2Im)]	1.93	0.92	4.2	45
[Fe(TTP)(2-MeHIm)]	1.95	0.85	4.2	45
[Fe(TTP)(1,2-Me_2Im)]	2.06	0.86	4.2	45
deoxymyoglobin	2.22	0.92	4.2	44
deoxyhemoglobin	2.40	0.92	4.2	44
Low-Spin Iron(II) Complexes				
[Fe(TMP)($Py)_2$]	1.24	0.45	4.2	46
[Fe(TPP)($Py)_2$]	1.15	0.40	77	47
[Fe(OEP)($Py)_2$]	1.13	0.46	4.2	48
[Fe(TPP)(1-VinIm)$_2$]	1.00	0.43	4.2	49
[Fe(TPP)($Pip)_2$]	1.44	0.51	4.2	50
[Fe(TpivPP)(1-MeIm)$_2$]	1.02	0.46	4.2	50
[Fe(TMP)(1-MeIm)$_2$][a]	1.11	0.45	77	51
[Fe(OEP)(1-MeIm)$_2$][a]	0.96	0.46	77	51
[Fe(TMP)(PMe_3)(1-MeIm)][a]	0.75	0.38	77	51
[Fe(TMP)($PMe_3)_2$][a]	0.47	0.36	77	51
[Fe(OEP)($PMe_3)_2$][a]	0.35	0.36	77	51

[a] In dimethylacetamide solution.